Performance of High-Convergence, Layered DT Implosions with Extended-Duration Pulses at the National Ignition Facility

V. A. Smalyuk,[1] L. J. Atherton,[1] L. R. Benedetti,[1] R. Bionta,[1] D. Bleuel,[1] E. Bond,[1] D. K. Bradley,[1] J. Caggiano,[1] D. A. Callahan,[1] D. T. Casey,[1] P. M. Celliers,[1] C. J. Cerjan,[1] D. Clark,[1] E. L. Dewald,[1] S. N. Dixit,[1] T. Döppner,[1] D. H. Edgell,[3] M. J. Edwards,[1] J. Frenje,[4] M. Gatu-Johnson,[4] V. Y. Glebov,[3] S. Glenn,[1] S. H. Glenzer,[1] G. Grim,[2] S. W. Haan,[1] B. A. Hammel,[1] E. P. Hartouni,[1] R. Hatarik,[1] S. Hatchett,[1] D. G. Hicks,[1] W. W. Hsing,[1] N. Izumi,[1] O. S. Jones,[1] M. H. Key,[1] S. F. Khan,[1] J. D. Kilkenny,[5] J. L. Kline,[2] J. Knauer,[3] G. A. Kyrala,[2] O. L. Landen,[1] S. Le Pape,[1] J. D. Lindl,[1] T. Ma,[1] B. J. MacGowan,[1] A. J. Mackinnon,[1] A. G. MacPhee,[1] J. McNaney,[1] N. B. Meezan,[1] J. D. Moody,[1] A. Moore,[1] M. Moran,[1] E. I. Moses,[1] A. Pak,[1] T. Parham,[1] H.-S. Park,[1] P. K. Patel,[1] R. Petrasso,[4] J. E. Ralph,[1] S. P. Regan,[3] B. A. Remington,[1] H. F. Robey,[1] J. S. Ross,[1] B. K. Spears,[1] P. T. Springer,[1] L. J. Suter,[1] R. Tommasini,[1] R. P. Town,[1] S. V. Weber,[1] and K. Widmann[1]

[1]*Lawrence Livermore National Laboratory, Livermore, California 94550, USA*
[2]*Los Alamos National Laboratory, Los Alamos, New Mexico 87545, USA*
[3]*Laboratory for Laser Energetics, University of Rochester, Rochester, New York 14623, USA*
[4]*Massachusetts Institute of Technology, Cambridge, Massachusetts 02139, USA*
[5]*General Atomics, San Diego, California 92121, USA*

(Received 14 May 2013; published 19 November 2013)

Radiation-driven, low-adiabat, cryogenic DT layered plastic capsule implosions were carried out on the National Ignition Facility (NIF) to study the sensitivity of performance to peak power and drive duration. An implosion with extended drive and at reduced peak power of 350 TW achieved the highest compression with fuel areal density of $\sim 1.3 \pm 0.1$ g/cm^2, representing a significant step from previously measured ~ 1.0 g/cm^2 toward a goal of 1.5 g/cm^2. Future experiments will focus on understanding and mitigating hydrodynamic instabilities and mix, and improving symmetry required to reach the threshold for thermonuclear ignition on NIF.

DOI: 10.1103/PhysRevLett.111.215001 PACS numbers: 52.57.Fg

The goal of inertial confinement fusion (ICF) [1,2] is to implode a spherical target to achieve high compression of the deuterium-tritium (DT) fuel and high temperature in the hot spot, to trigger ignition and produce significant thermonuclear energy gain. In the pioneering work by Nuckolls *et al.*, the first laser-fusion designs were based on 1-kJ of laser energy [3]. In laser fusion, the objective is to achieve sufficiently high fuel areal densities, while the confinement time is determined by the inertia of the fuel and shell. An extremely high degree of drive uniformity and symmetry is required for these high convergence, high density, low fuel entropy (adiabat) implosions [3]. The two main approaches for laser fusion are direct and indirect drive [1,2]. In direct drive, the spherical targets are directly driven with the laser light [1], while in indirect drive the laser light is converted to x rays (produced in a high-Z cavity called a hohlraum) to drive the implosions [2,4]. Direct drive should be more energy efficient than indirect drive, while high uniformity should be more easily achieved with indirect drive [5]. Precise pulse shaping is necessary to time the shocks in the drive, and hot-electron preheat needs to be kept low to keep the fuel on a low adiabat for high compression [4].

In the current indirect drive point design at the National Ignition Facility (NIF) [6,7] with a plastic ablator, the fuel reaches a peak implosion velocity of ~ 360 km/s, driven with a 1.6 MJ laser pulse at peak power of 410 TW. To achieve high compression, the entropy in the surrounding DT fuel must remain low to reach high density with the available laser energy [2]. The DT fuel entropy is often characterized by the adiabat $\alpha = P/P_{\mathrm{cold}}$, the ratio of the plasma pressure P to the Fermi pressure of a fully degenerate gas P_{cold}. In the NIF point design, the adiabat α is low, $\alpha \sim 1.4$, to achieve high compression of the surrounding DT fuel and the predicted neutron yield of ~ 20 MJ [7,8]. Figure 1 shows simulated [7] shell density profiles for an ignition design at radius of $R \sim 1000$ μm (the initial size of the capsule), $R \sim 200$ μm near peak velocity, and $R \sim 30$ μm which corresponds to the onset of ignition. The electron temperature profile at the onset of ignition is also shown. In this design, the peak DT fuel density increases by more than a factor of 1000, before the onset of ignition. The implosion must achieve a temperature of $T_e > 5$ keV in the central hot spot, with hot-spot areal density of $\rho R_{\mathrm{hotspot}} \sim 0.3$ g/cm^2, surrounded by a dense main fuel layer with $\rho R_{\mathrm{fuel}} \sim 1.5$ g/cm^2 [7]. The areal density is one of the fundamental quantities in ICF, it is part of the generalized Lawson criterion $(\rho R/1.5)^{0.8} \times (T/3.8)^{1.8} > 1$, expressed in terms of measurable ICF parameters ρR (in units of g/cm^2) and temperature T

 © 2013 American Physical Society

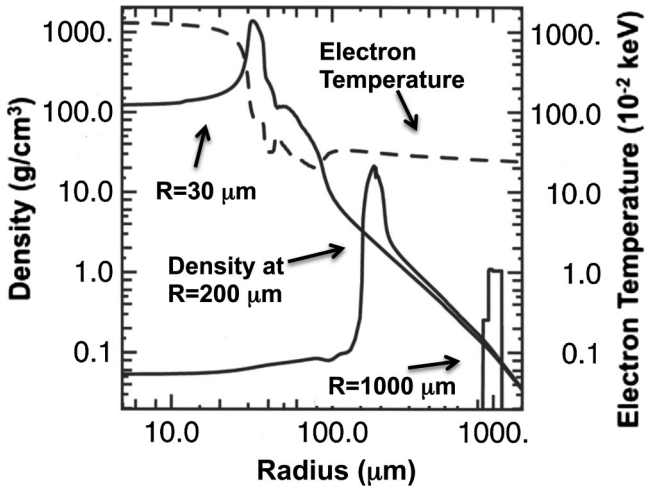

FIG. 1. Shell density profiles (solid curves) are shown as a function of shell radius at initial position (right-hand side curve), during implosion at radius of 200 μm (middle curve), and at the onset of ignition at a radius of 30 μm (left-hand side) with an electron temperature profile at the onset of ignition shown by a dashed curve.

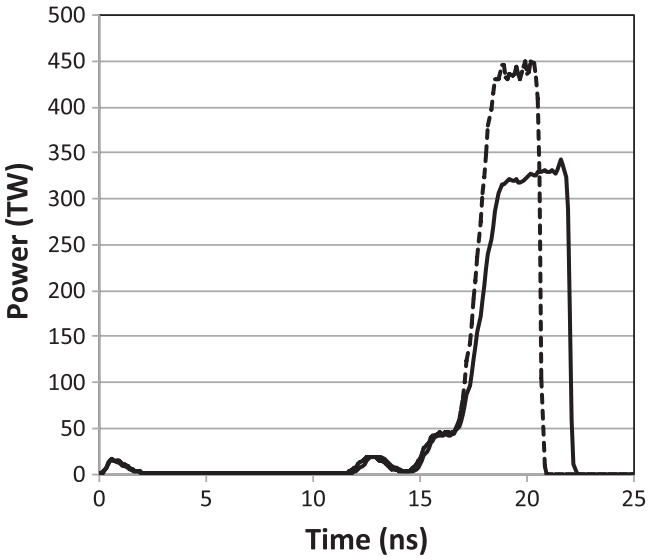

FIG. 2. A comparison of the extended-duration laser pulse used in shot N120321 with peak power of 350 TW and energy of 1.6 MJ (solid curve) and the nominal-duration pulse with peak power of 450 TW and energy of 1.5 MJ (dashed curve, shot N111215 [17]).

(in units of keV) [8]. Hence, achieving high fuel areal density is a key objective for ICF.

In 1988, the fuel areal densities up to $\sim$0.05 g/cm^2 were achieved in cryogenic, layered DT, directly driven implosions on the 24-beam OMEGA laser system using 0.351-μm laser drive with total energies up to $\sim$1.5 kJ and simple Gaussian 0.7-ns pulses [5]. In 2002, the first experiments on the more powerful 60-beam OMEGA laser system produced areal densities of $\sim$0.06 g/cm^2 using cryogenic D_2 layered implosions with total laser energies up to 23 kJ [9]. These experiments were performed with 1-ns square pulses, without sophisticated pulse shaping, resulting in a relatively high fuel adiabat of $\sim$25. In 2008, the fuel adiabat was decreased to $\sim$2.5 using shaped pulses, resulting in increased areal densities of $\sim$0.2 g/cm^2 achieved using drive energies of $\sim$16 kJ in cryogenic D_2 layered implosions on OMEGA [10]. More recent 2009 experiments with "triple-picket" shaped pulses achieved the highest compression on OMEGA with areal densities up to $\sim$0.3 mg/cm^2 in layered DT implosions at laser energies of 25 kJ [11]. These experiments demonstrated that high areal densities can be achieved in conditions of low hot-electron preheat [12,13] using sophisticated pulse-shaping techniques to keep the fuel at low adiabats [10,11].

The first NIF experiments with cryogenic DT layers in 2010 achieved fuel areal densities of $\sim$0.6 g/cm^2 with indirectly driven implosions using Au hohlraums at a laser energy of $\sim$1.1 MJ and peak laser power of $\sim$300 TW [14]. The fuel adiabat was set by a series of four staged shocks in these implosions [15]. Shock-tuning experiments discovered that the shock mistiming caused by ice deposition in the hohlraum laser entrance hole (LEH) windows raised the fuel adiabat in these first NIF layered implosions [16]. In further experiments where the ice buildup problem was eliminated and following a shock-tuning campaign [15], the fuel areal densities were increased to $\sim$1 g/cm^2 using laser energies up to 1.6 MJ and peak powers up to $\sim$450 TW [14]. In these cryogenic DT implosions, the implosion velocities and fuel compressions were lower than predicted, indicating an overall $\sim$15% reduction in x-ray drive [17,18]. The x-ray drive deficit appears to have been especially pronounced during the "coasting" phase after the laser drive was turned off, typically at a shell convergence ratio of $\sim$2, corresponding to an outer shell radius of $R \sim 500$ μm [19,20]. The reduction in x-ray drive during the coasting phase also led to shell decompression, lower shell convergence, and reduced compression of the DT fuel [20]. Hot-electron preheat is thought to have a negligible (a few percent) contribution to this compression degradation [21].

This Letter describes results of implosions with new, lower power, extended-duration laser drives intended to reduce the duration of the coasting phase, and therefore improve fuel compression. Figure 2 shows the extended-duration laser pulse used in this implosion with a peak power of $\sim$350 TW and a total laser energy of $\sim$1.6 MJ for the shot N120321, compared to a typical nominal-duration, higher-power pulse at similar energy of $\sim$1.5 MJ, used in earlier experiments (shot N111215) [17]. The pulses were turned off later, when the outer shell is at radius $R \sim 300$ μm. The implosions using the lower power, extended drives achieved the highest fuel compression with areal density up to $\sim 1.3 \pm 0.1$ g/cm^2,

representing a significant improvement over the previous results of ~1.0 g/cm^2, and approaching the ignition requirement of 1.5 g/cm^2. As the achieved fuel compression was very close to the requirement, the main focus of future experiments will be shifted towards mitigating hydrodynamic instabilities and mix, and reducing asymmetries, to increase yield and to enter the alpha-heating (''boot strapping'') regime.

These new ''no-coast'' experiments correspond to ten implosions with new extended-duration drives performed at peak laser powers ranging from ~290 to ~400 TW and total laser energies from ~1.5 to ~1.7 MJ. The capsule, target, and drive parameters varied slightly in these implosions including ablator thickness, Si dopant concentration, hohlraum material (gold vs uranium), surface and ice roughnesses, and details of the pulse shapes. We focus here on the highest compression shot N120321. Capsule and hohlraum details in this shot were described previously (Fig. 1 of Ref. [17]), with the exceptions that the Si concentration was doubled in all Si-doped layers, and the hohlraum was made of uranium with a gold lining. A plastic ablator had a 195-μm wall thickness and 2280-μm-initial outer diameter, within which a 69 μm thick cryogenic DT layer was grown. The U hohlraum produces higher drive at peak power, while the inner Au layer provides oxidation protection for the U [22,23]. The laser is calculated to be absorbed in the Au layer, and does not directly interact with the U, whereas the U increases the opacity in the wall, which decreases the wall losses and increases peak radiation temperature. The extended ''no-coast'' pulse was turned off when the outer shell radius was predicted to be $R \sim 300$ μm to minimize the coasting phase, while the nominal-duration pulse was turned off at $R \sim 500$ μm.

Table I summarizes the measured and predicted drive and performance results for shot N210321. The simulated adiabat was close to the ignition specification of ~1.4, while the predicted fuel velocity was 320–330 km/s. The roughnesses of the plastic capsule surface and ice layer were comprehensively characterized, and were close to specifications [8]. The DT ice roughness power spectrum met the requirements for all modes except for mode 1 on shot N120321, where it was ~2 times higher than the requirement. The effects of ice surface grooves [24] can be characterized by using a parameter K, defined as a sum over all defects with area A and length L as

$$K = \sqrt{\frac{1}{V_{\text{fuel}}} \sum_{i=1}^{n} A_i^2 L_i},$$

where V_{fuel} is the volume of the DT fuel [7]. Experimental specifications [8] have been set requiring $K < 0.70$ μm, and the largest groove area A required to be <200 μm^2. For the N120321 shot, the K value was measured to be 0.70 μm and the largest groove area was 153 μm^2, meeting the experimental requirement. The dust particles on the outer surface were also characterized. Although specifications required that no single particle with a volume greater than 30 μm^3 should be present on a capsule surface [7], this capsule had one particle that was about a factor of 2 outside this requirement.

The performance of all cryogenic DT layered implosions on NIF has been characterized with a comprehensive set of nuclear and x-ray diagnostics [25,26]. The measured peak temperature was 307 ± 4 eV, while the implosion bang time was 22.84 ± 0.04 ns. X-ray images of the imploded core emission showed good symmetry of the emitting hot spot [27]. The hot-spot distortion requirement was <25% rms [7] for the deviation from round of the emission contour at 17% of the peak brightness. The measured hot-spot distortion was small, 16% ± 4% rms, although cold-shell symmetry (not measured in these shots) might also be an important factor [28]. Fuel compression was inferred using the down-scattered ratio (DSR) of scattered neutrons in the range from 10 to 12 MeV relative to primary neutrons in the range from 13 to 15 MeV [29]. The down-scattered neutrons determining DSR are mostly scattered in the DT fuel, and in simulations DSR is proportional to the fuel areal density: ρR(g/cm^2) ~ 21 × DSR [29,30]. This shot had very good overall performance and the highest fuel areal density observed to date: neutron yield of 4.2 ± 0.1 × 10^{14}, ion temperature of 3.1 ± 0.1 keV, and DSR of 6.3 ± 0.5%, corresponding to a fuel areal density of ~1.3 ± 0.1 g/cm^2.

TABLE I. Key experimental results and predictions using 1D, 2D, and 3D simulations for the shot N120321 with peak laser power of 350 TW and energy of 1.6 MJ.

	N120321, 350 TW peak power			
	1D	2D	3D	Exp.
Fuel velocity (km/s)	319.7	332	332	···
Remaining ablator (%)	11.8	8.9	8.9	···
Fuel adiabat	1.43	1.46	1.46	···
DSR (%)	6.44	6.2	6.0	6.3 ± 0.5
Ion temperature (keV)	3.14	3.21	3.8	3.1 ± 0.1
Neutron yield (10^{14})	37	20.9	13.0	4.2 ± 0.1
Measured yield over prediction (%)	11.4 ± 0.3	20.1 ± 0.5	32.3 ± 1.0	···

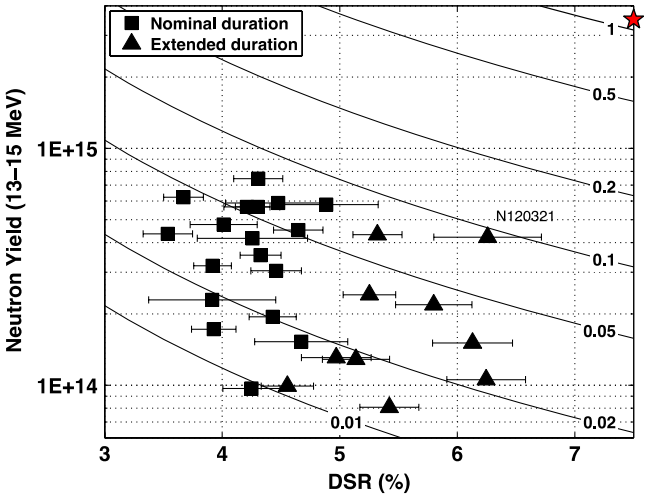

FIG. 3 (color online). Measured DT neutron yield in the range from 13 to 15 MeV plotted against measured neutron down-scattered-ratio DSR for extended-duration cryogenic DT implosions on NIF (triangles) and all other previous implosions (squares). Solid curves represent contours of the net performance parameter ITFX ranging from 0.01 to 1. The star represents the region above the ignition threshold with ITFX of 1.

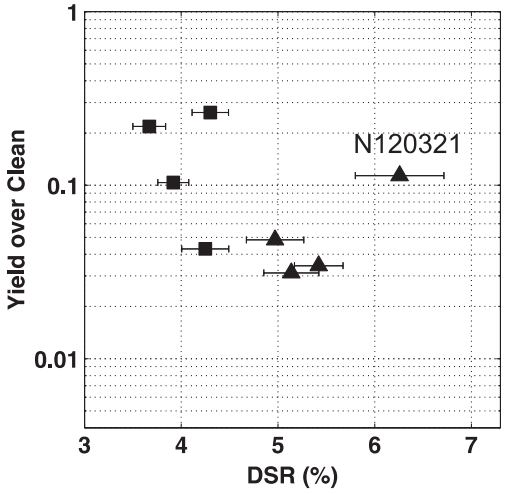

FIG. 4. Measured DT neutron yield over predicted by 1D simulations (yield over clean) against measured DSR for extended-duration implosions (triangles) and nominal-duration implosions (squares). One-dimensional predictions do not include effects of alpha heating; therefore, measured yield degradations are due to only hydrodynamic instabilities and asymmetries.

Figure 3 shows the performance of the extended duration shots (triangles) compared to all other layered DT NIF shots (squares). Solid and dashed curves are contours of constant ignition threshold factor (ITFX), defined as $\mathrm{ITFX} = (\frac{Y_{\mathrm{DT}}}{4.0e15})(\frac{\mathrm{DSR}}{0.067})^{2.1}$, where Y_{DT} is the measured DT yield in the primary 13–15 MeV range [7]. In simulations, ITFX is a good measure of how close an implosion is to the threshold for thermonuclear ignition [8]. Shot N120321 provided the highest DSR observed to date and an ITFX of ~0.1. The majority of the experiments with the extended-duration pulses had higher measured compression than the normal drive duration implosions [14,31]. Measured peak implosion velocities were ~10% higher with extended pulses [18], contributing to the measured ~30% increase in the fuel areal density. Improved shock tuning [32] and generally lower hot-electron preheat (due to generally lower peak laser power) may also have contributed to the lower fuel adiabat resulting in higher compression, although reduced hot-electron preheat was expected to have a small effect on the fuel areal-density [21].

As shown in Fig. 4, the measured DT neutron yield over predicted by 1D simulations (yield over clean) was below ~30% for moderate-compression implosions with DRS ~4%. Simulations were performed for a subsection of shots shown in Fig. 3. In the new high-compression implosions, YOCs were in the range from ~3 to ~10% with the highest YOC of ~11% achieved in the shot N120321. One-dimensional predictions in Fig. 4 do not include effects of alpha heating; therefore, measured yield degradations are due to only hydrodynamic instabilities and asymmetries. The measured yields over those predicted by 2D and 3D simulations (intended to explain the degradation due to hydrodynamic instabilities) were in the range from ~4 to ~30%, indicating a need to improve modeling capabilities. Amounts of measured ablator-fuel mix were also correlated with the yield degradation in these high-compression implosions [33]. In the shot N120321, the fuel areal density of ~1.3 g/cm^2 (corresponding to DSR of ~6.3%) has been achieved with fuel velocity of ~330 km/s. While these two key performance parameters were close to the goals of the of the point design, 1.5 g/cm^2 (DSR of ~7%) and ~360 km/s, respectively, the YOC was ~4 times below the value of ~40%, necessary for ignition [7]. As the achieved fuel compression was very close to the requirement (see Fig. 3), the main focus of the ignition program has shifted towards understanding and mitigating hydrodynamic instabilities and mix, reducing asymmetries, to increase YOC toward a value of ~40% and to enter the alpha-heating (boot strapping) regime. Instability-growth experiments are underway at NIF to understand the physics of unstable growth at the ablation front, and techniques to probe the ablator-ice interface, and the inner-ice surface are being explored.

In conclusion, experiments with an extended-duration drive achieved the highest compression in implosions with x-ray driven CH capsules containing cryogenic DT layers. Future experiments will focus on reducing hot-spot mix and increasing neutron yield performance close to a goal of ~40% of the 1D predictions (without effects of alpha heating) while keeping the peak fuel velocity and the fuel areal density close to the ignition requirements to reach the threshold for ignition on NIF.

This work was performed under the auspices of the U.S. Department of Energy by Lawrence Livermore National Laboratory under Contract No. DE-AC52-07NA27344.

[1] S. Atzeni and J. Meyer-ter-Vehn, *The Physics of Inertial Fusion: Beam Plasma Interaction, Hydrodynamics, Hot Dense Matter*, International Series of Monographs on Physics (Clarendon Press, Oxford, 2004).
[2] J. D. Lindl, *Inertial Confinement Fusion: The Quest for Ignition and Energy Gain Using Indirect Drive* (Springer-Verlag, New York, 1998).
[3] J. Nuckolls, L. Wood, A. Thiessen, and G. Zimmerman, Nature (London) **239**, 139 (1972).
[4] J. Nuckolls, Phys. Today **35**, No. 9, 24 (1982).
[5] R. L. McCrory *et al.*, Nature (London) **335**, 225 (1988).
[6] E. I. Moses, R. N. Boyd, B. A. Remington, C. J. Keane, and R. Al-Ayat, Phys. Plasmas **16**, 041006 (2009); G. H. Miller, E. I. Moses and C. R. Wuest, Opt. Eng. (N.Y.) **43**, 2841 (2004).
[7] S. W. Haan *et al.*, Phys. Plasmas **18**, 051001 (2011).
[8] B. K. Spears and J. Lindl, Phys. Plasmas (to be published).
[9] T. C. Sangster *et al.*, Phys. Plasmas **10**, 1937 (2003).
[10] T. C. Sangster *et al.*, Phys. Rev. Lett. **100**, 185006 (2008).
[11] V. N. Goncharov *et al.*, Phys. Rev. Lett. **104**, 165001 (2010).
[12] W. L. Kruer, *The Physics of Laser Plasma Interactions* (Addison-Wesley, Reading, MA, 1988).
[13] V. A. Smalyuk *et al.*, Phys. Rev. Lett. **100**, 185005 (2008).
[14] A. MacKinnon *et al.*, Phys. Rev. Lett. **108**, 215005 (2012).
[15] H. F. Robey *et al.*, Phys. Rev. Lett. **108**, 215004 (2012).
[16] H. F. Robey *et al.*, Phys. Plasmas **19**, 042706 (2012).
[17] S. H. Glenzer *et al.*, Phys. Plasmas **19**, 056318 (2012).
[18] D. G. Hicks *et al.*, Phys. Plasmas **19**, 122702 (2012).
[19] D. A. Callahan *et al.*, Phys. Plasmas **19**, 056305 (2012).
[20] D. S. Clark *et al.*, Phys. Plasmas **20**, 056318 (2013).
[21] T. Döppner *et al.*, Phys. Rev. Lett. **108**, 135006 (2012).
[22] N. B. Meezan *et al.*, Phys. Plasmas **20**, 056311 (2013).
[23] J. L. Kline *et al.*, Phys. Plasmas **20**, 056314 (2013).
[24] B. J. Kozioziemski *et al.*, Fusion Sci. Technol. **59**, 14 (2011).
[25] M. J. Edwards *et al.*, Phys. Plasmas **18**, 051003 (2011).
[26] S. H. Glenzer *et al.*, Phys. Rev. Lett. **106**, 085004 (2011).
[27] S. Glenn *et al.*, Rev. Sci. Instrum. **83**, 10E519 (2012).
[28] R. H. H. Scott *et al.*, Phys. Rev. Lett. **110**, 075001 (2013).
[29] J. A. Frenje *et al.*, Rev. Sci. Instrum. **79**, 10E502 (2008).
[30] O. S. Jones *et al.*, Phys. Plasmas **19**, 056315 (2012).
[31] O. L. Landen *et al.*, Plasma Phys. Controlled Fusion **54**, 124026 (2012).
[32] H. F. Robey *et al.*, Phys. Plasmas **20**, 052707 (2013).
[33] T. Ma *et al.*, Phys. Rev. Lett. **111**, 085004 (2013).